Priming programed Mucosal-Associated Invariant T cells protect against systemic or local bacterial infection

Zhe Zhao
University of Melbourne https://orcid.org/0000-0003-1009-324X
Mai Shi
University of Melbourne
Tianyuan Zhu
University of Melbourne
Huimeng Wang
University of Melbourne
Troi Pediongco
University of Melbourne
Xin Yi Lim
Department of Microbiology and Immunology, The University of Melbourne https://orcid.org/0000-0002-9806-5894
Bronwyn Meehan
Peter Doherty Institute for Infection and Immunity at The University of Melbourne
Adam Nelson
University of Melbourne
David Fairlie
University of Queensland https://orcid.org/0000-0002-7856-8566
Jeffrey Mak
Institute for Molecular Bioscience, The University of Queensland https://orcid.org/0000-0002-8011-4539
Sidonia Eckle
Peter Doherty Institute for Infection and Immunity at The University of Melbourne
https://orcid.org/0000-0003-0766-171X
Jamie Rossjohn
Monash University https://orcid.org/0000-0002-2020-7522
James McCluskey (jamesm1@unimelb.edu.au)
University of Melbourne https://orcid.org/0000-0002-8597-815X
Alexandra Corbett
The University of Melbourne https://orcid.org/0000-0003-1618-4337

Zhenjun Chen
University of Melbourne https://orcid.org/0000-0003-1205-683X

Article

Keywords: MAIT, mucosal-associated invariant T, antibacterial function

Posted Date: July 15th, 2020

DOI: https://doi.org/10.21203/rs.3.rs-39302/v1

Version of Record: A version of this preprint was published at Nature Communications on July 16th, 2021. See the published version at https://doi.org/10.1038/s41467-021-24570-2.

Priming programed Mucosal-Associated Invariant T cells protect against systemic or local bacterial infection

Authors

Zhe Zhao[1]†, Mai Shi[1,2]†, Tianyuan Zhu[1,2], Huimeng Wang[1,3], Troi Pediongco, Xin-Yi Lim[1], Bronwyn S Meehan[1], Adam G. Nelson[1], David P Fairlie[4,5], Jeffrey Y. W. Mak[4,5], Sidonia BG Eckle[1], Jamie Rossjohn[6,7,8], James McCluskey[1]*, Alexandra J Corbett[1]†* and Zhenjun Chen[1]†*

Affiliations

[1]Department of Microbiology and Immunology, The University of Melbourne, Peter Doherty Institute for Infection and Immunity, Melbourne, Australia.

[2]School of Medicine, Tsinghua University, Beijing, China

[3]State Key Laboratory of Respiratory Disease, Guangzhou Institute of Respiratory Disease, The First Affiliated Hospital of Guangzhou Medical University, Guangzhou, Guangdong 510182, China.

[4]Division of Chemistry and Structural Biology, Institute for Molecular Bioscience, The University of Queensland, Brisbane, Australia.

[5]Australian Research Council Centre of Excellence in Advanced Molecular Imaging, The University of Queensland, Brisbane, Australia.

[6]Infection and Immunity Program and the Department of Biochemistry and Molecular Biology, Biomedicine Discovery Institute, Monash University, Clayton, VIC 3800, Australia.

[7]Australian Research Council Centre of Excellence in Advanced Molecular Imaging, Monash University, Clayton, VIC 3800, Australia.

[8]Institute of Infection and Immunity, Cardiff University, School of Medicine, Heath Park, CF14 4XN Wales, UK.

†These authors contributed equally to this work.

*Materials and Correspondence: James McCluskey jamesm1@unimelb.edu.au
Z Chen zhenjun@unimelb.edu.au, http://orcid.org/0000-0003-1205-683X
AJ Corbett corbetta@unimelb.edu.au, http://orcid.org/0000-0003-1618-4337

Running title: MAIT-1 cell-mediated protection against different bacterial infections

ABSTRACT

Mucosal-Associated Invariant T (MAIT) cells have potent antibacterial functions. Their protective capacity, *in vivo*, has been demonstrated in mouse models, particularly of respiratory infections. We now show that during systemic infection of mice with *Francisella tularensis* Live Vaccine Strain (LVS), MAIT cell expansion was evident in the liver, lungs, kidney, spleen and blood. MAIT cells manifested a polarised T_h1-like (termed "MAIT-1") phenotype and cytokine profile that conferred a critical role in controlling bacterial load. After resolution of the primary infection, the expanded MAIT cells developed to a stable memory-like MAIT-1 cell population, suggesting a basis for vaccination and protection against subsequent challenge. Indeed, a systemic vaccination with synthetic ligand (5-OP-RU) in combination with CpG adjuvant boosted MAIT-1 cells and resulted in enhanced protection against systemic and local infections with *F. tularensis* and *Legionella longbeachae*. Our study highlights the potential utility of targeting MAIT cells to combat multiple bacterial pathogens.

INTRODUCTION

Microbial infections in patients with compromised immunity (e.g. organ transplant recipients), particularly with multi-drug resistant pathogens, cost several billion dollars each year[1, 2, 3]. Bacterial sepsis is associated with a very high mortality of 30% to 50% [4, 5] and is estimated to cause 6 million deaths among 30 million people affected worldwide every year[6] , making it a leading cause of death in hospitals. Thus, there is great interest in the development of new preventive and therapeutic approaches, including T cell-based vaccination[7]. Although some progress has been made in this area, complete protection by T cell vaccines has not yet been achieved and there remains a great need to understand the generation of effective T cell memory and responses[7].

Mucosal-Associated Invariant T (MAIT) cells are an abundant αβ T cell subset (averaging 3% of T cells in human blood[8]) that express semi-invariant T cell antigen receptors (TCRs), comprising TRAV1-2-TRAJ33/12/20 in humans[9, 10, 11] or TRAV1-TRAJ33 (Vα19-Jα33) in mice, paired with a limited TCR β chain repertoire. MAIT cells recognise conserved vitamin B2 metabolite-based antigens (Ag) from microbes, presented by the Major histocompatibility complex (MHC) Class I related protein 1 (MR1) molecule. Riboflavin biosynthesis, the source of MAIT cell Ag, is an essential and highly conserved metabolic pathway present in a diverse range of bacteria and yeasts. We and others have shown in mouse models, that MAIT cells afford a protective function against several bacterial pathogens[12, 13, 14, 15, 16, 17], including respiratory infections with *Legionella longbeachae*[12] and *Francisella tularensis*[13]. Human *in vitro* studies demonstrated reactivity of MAIT cells to an even broader range of microbial species, reviewed in [14], including *Streptococcus* spp.[15, 16],

Shigella flexneri[17] and fungal pathogens *Aspergillus fumigatus*[18] and *Candida albicans*[19]. Alterations in MAIT cell frequency and function have been reported in patients with tuberculosis[20, 21, 22] and other infectious diseases[23, 24, 25, 26, 27]. Sandburg and colleagues reported a patient with cystic fibrosis affected by recurrent, and eventually fatal, bacterial infections which correlated with a striking lack of detectable circulating MAIT cells[24].

Despite the presence of MAIT cells at many sites[28], including high numbers in the liver [29], female reproductive tract[30] and intestine[31], previous studies have mostly examined their protective role in local infections[13, 32]. Thus far, a protective role has been demonstrated most convincingly in respiratory infections[12, 13], with little definitive *in vivo* evidence to date of their capacity to contribute to protective immunity against systemic infection. *Francisella tularensis* causes both respiratory disease and tularemia, a rare but often fatal systemic infection. Infection can occur via the respiratory route, by ingestion of contaminated water or via tick bites[33]. *F. tularensis* LVS was developed as a vaccine strain with reduced pathogenicity[34]. Although its use in humans was discontinued due to the risks associated with administration of a live organism with undetermined genetics, *F. tularensis* LVS provides a useful model for pathogenicity and immune response research[35], and was previously used to demonstrate a protective role for MAIT cells during respiratory infection[13, 36].

Here, we examined the role of MAIT-1 cells in a systemic infection model of *F. tularensis* LVS infection, where the kinetics of the MAIT-1 cell response was investigated in multiple organs. MAIT-1 cells were highly responsive and were not only critical to controlling bacterial load, but also formed a "memory-like" population after infection. Vaccination with synthetic 5-OP-RU antigen in combination with CpG adjuvant recapitulated this expanded memory MAIT-1 cell population and afforded better control of subsequent systemic and local infections by both *F. tularensis* and *L. longbeachae*.

RESULTS

F. tularensis LVS activates MAIT reporter cells *in vitro* in an MR1-dependent manner and induces a systemic MAIT cell response *in vivo*.

To confirm that *F. tularensis* LVS, riboflavin biosynthesis proficient bacteria as shown in the Kyoto Encyclopedia of Genes and Genomes database, can stimulate MAIT cells, we used an *in vitro* activation assay with Jurkat.MAIT reporter cells expressing a TRAV1-2/TRBV6-1 TCR (Jurkat.MAIT-AF7)[11] co-cultured with C1R.hMR1 cells as APCs, as previously described[11]. *F. tularensis* bacterial lysate was able to stimulate Jurkat.MAIT-AF7 cells in this assay as assessed by up-regulation of cell surface CD69 expression (**Fig. 1, A**). Anti-MR1 monoclonal antibody (mAb)

(26.5), but not an isotype control mAb, completely blocked this response, consistent with MR1-dependent activation. Like previous studies using other bacteria[22, 37] and consistent with MAIT cell expansion in the lungs in respiratory *F. tularensis* infection[13] these data demonstrated that *F. tularensis* LVS is capable of producing Ags that stimulate MAIT cells in an MR1-dependent manner.

To examine the MAIT cell response *in vivo*, C57BL/6 mice were infected with *F. tularensis* LVS intravenously (i.v) with a sublethal dose of 10^4 colony forming units (CFU). MAIT cell frequencies and numbers were assessed in a range of organs (liver, lungs, spleen, kidneys) and in the blood by MR1:5-OP-RU tetramer staining (**Supplementary Fig. 1**). Significant MAIT cell expansion was observed in all organs tested and in the blood at 14 days post infection (dpi), compared to uninfected mice **(Fig. 1, B-D)**. Non-MAIT αβ T cells were also increased in response to infection, as expected (**Fig. 1, E**), but their increase was less pronounced as compared to that seen for MAIT cells. Since *F. tularensis* infection can occur naturally through inhalation, wounds or tick bites, we next tested various infection routes: intranasal, intratracheal, intraperitoneal (i.p.) and subcutaneous (s.c.), using a range of doses for each. Regardless of the infection route, systemic dissemination occurred resulting in significant MAIT cell accumulation in all tested organs in mice infected with sufficient dose (**Supplementary Fig. 2**). Due to the ease of consistent and accurate delivery of inoculum, and rapid dissemination of bacteria, we chose the i.v. route for all following infection experiments.

The MAIT cell expansion following *F. tularensis* infection is rapid and long-lasting in all organs

Upon *F. tularensis* LVS infection, a typical valley shaped-weight change was recorded in infected mice (**Fig. 2, H**) with mice losing weight until day 5, then recovering and reaching their starting weight by day 12. The bacteria clearance kinetics showed an initial decline in the bacterial load in the blood, but expansion at early stages in all other sites, which reached a plateau around 3 dpi, followed by clearance (undetectable level) within 12 days (**Fig. 2, A**).

We next investigated the kinetics of MAIT cell expansion in various organs. Both the frequency (relative to total αβ-T cells, **Fig. 2, B**) and number (**Fig. 2, C-G**) of MAIT cells increased significantly in the early stages of the infection time-course. Remarkably, by day 6 MAIT cells represented ~29% of αβ-T cells in the liver, 27% in the lungs, 26% in the kidneys, 19% in the blood and 16% in the spleen. The frequency of MAIT cells reached a plateau between 9-14 dpi in the liver, lungs and kidney, in contrast to the total number, which plateaued at about 6 dpi in all organs. Interestingly, high frequencies of MAIT cells (43% in the liver, 8% in the lungs, 21% in the kidneys 4% in the blood and 2% in the spleen) were maintained at 100 dpi, long after clearance of bacteria to undetectable numbers. This was in contrast to non-MAIT αβ-T cells, which contracted as expected to their

homeostatic level (in numbers) in all organs (**Fig. 2, C-G**).

***F. tularensis* infection polarizes MAIT cells to a MAIT-1 (Th1 like) functional phenotype.**

We next examined the functional phenotype of the MAIT cell populations that were expanded during *F. tularensis* infection by assessing their cytokine profile during the acute infection phase (6 dpi) and the expression of transcription factors in MAIT cells from naïve mice and at representative time points of acute infection (6 dpi), recent bacterial clearance (14 dpi) and memory phase (100 dpi). Four cytokines, TNF, IFNγ, GM-CSF, and IL-17, previously shown to be produced by mouse and human MAIT cells[12, 37, 38, 39], were examined directly *ex vivo*. The majority of MAIT cells were found to be polarized to a Th1 like phenotype, with high proportions, and numbers, of cells expressing TNF, IFNγ and GM-CSF, but few detectable IL-17-producing cells during the acute phase of infection (6 dpi) (**Fig. 3 and Supplementary Fig. 3, 4**). Interestingly, MAIT cells appeared to produce these Th1 cytokines in an organ specific pattern, with kinetic differences in the proportions of cells producing each cytokine. This was particularly apparent late in infection, with consolidation and persistence of population of MAIT-1 cells in the liver and spleen, but a reduction of MAIT-1 proportion in the lung and kidney (**Fig. 3, B-C)**. This was most evident for IFNγ-producing MAIT cells (**Fig. 3, B**), with TNF-producing MAIT cells displaying a similar but less pronounced pattern (**Fig. 3, C)**, and the abundance of GM-CSF-producing MAIT cells increasing throughout the infection in all organs except for the kidney (**Fig. 3, C)**. In contrast, the proportion of IL-17-producing MAIT-17 cells declined in both liver and lungs (**Fig. 3, C)**, but was later increased in the lungs. The frequencies of cytokine producing non-MAIT αβ-T cells were generally lower compared to MAIT cells and there was no clear pattern of changes over time, although IFNγ production was the most abundant, particularly in the early stages of infection (**Fig. 3A-C**).

The production of Th1 and Th17 cytokines by MAIT cells were consistent with their expression of the closely correlated transcription factors T-bet and RORγt, respectively. We found that naïve pulmonary MAIT cells were predominantly (>80%) T-bet$^-$ RORγt$^+$ (MAIT-17) (**Fig. 4**), consistent with our previous study[12], whereas in the liver >60% had a MAIT-1 phenotype (RORγt$^-$ T-bet$^+$) and there was a mixture of MAIT-1 and MAIT-17 cells in the kidney, spleen and blood (**Fig. 4**). Following infection (6 dpi) with *F. tularensis*, almost all MAIT cells were RORγt$^-$T-bet$^+$ in all organs and in the blood (**Fig. 4**). Remarkably, at 100 dpi, long after bacteria were cleared to undetectable levels **(Fig. 2, B)**, the phenotype of MAIT cells remained skewed towards MAIT-1. However, there was some shift in phenotype by this time towards the naïve phenotype in each organ consistent with the results seen in with intracellular cytokine staining (**Fig. 3, B-C**). This was most evident in the lungs, and suggested an organ-specific milieu may exist, which drives differently skewed responses (**Fig. 4**).

Overall, our data suggest that tissue-specific signals foster different polarization of MAIT cells at different sites. During infection, these are overruled by pathogen-derived signals, and long term after infecting the resultant MAIT cells are shaped by the balance of these factors.

MAIT-1 cells are critical for controlling bacteria during *F. tularensis* systemic infection.

Next we examined the protective role of MAIT-1 cells in *F. tularensis* systemic infection by comparing WT (C57BL/6) mice with *Mr1*$^{-/-}$ mice, which lack MAIT cells. Following inoculation of mice i.v. with 10^4 CFU *F. tularensis* LVS, significantly higher bacterial loads were observed at 6 dpi in all organs (liver, lung, spleen kidney and blood) of *Mr1*$^{-/-}$ mice than in WT mice, and the difference was also significant at 5 dpi and 7 dpi in some organs (**Fig. 5, A-E**). In these experiments, bacteria were cleared to undetectable levels by day 12 post infection either with or without MAIT cells. However, when a higher infection dose ($3x10^4$ CFU) was used, *Mr1*$^{-/-}$ mice showed significantly poorer survival (based on humane endpoints outlined in methods) (**Fig. 5, F**), suggesting that MAIT-1 cells play a protective role, which can be critical for controlling bacterial growth even when other arms of the immune system are intact.

We next tested the protective role of MAIT-1 cells in a more severe infection setting. The peritoneal cavity contains only a small number of immune cells[40] and intraperitoneal inoculation of WT mice with *F. tularensis* can cause severe infection and death in some mice with as few as 50 CFU (**Supplementary Fig. 5, B**). Here, adoptive transfer of MAIT-1 cells was conducted to WT mice, followed by bacterial challenge with 10 CFU *F. tularensis* LVS (**Supplementary Fig. 5, A-B**). Transferred MAIT cells were sorted from the livers of mice infected with *F. tularensis* to boost MAIT cell numbers. When adoptively transferred, these cells provided dose-dependent protection with full protection achieved when 5×10^5 MAIT cells were transferred (**Supplementary Fig. 5, B**).

To further test the capacity for MAIT-1 cells to provide protection, we then moved to an immune compromised setting and utilized *Rag2*$^{-/-}\gamma C^{-/-}$ mice, which lack T, B, and NK cells[41]. These mice are severely immune compromised and as expected all mice succumbed to a low dose of *F. tularensis* LVS (20 CFU) i.v. within 20 dpi (**Fig. 6C**). For these experiments, we sourced MAIT-1 cells for adoptive transfer from the livers of WT mice primed with synthetic 5-OP-RU Ag and CpG adjuvant (**Fig. 6, A**) to ensure no carry over of live bacteria to the recipient mice before challenge. This priming method recapitulated the predominant MAIT-1 phenotype in the liver as seen with *F. tularensis* infection (**Fig. 6, A**). Mice receiving adoptively transferred MAIT cells were able to significantly prolong survival after subsequent i.v. challenge with *F. tularensis* LVS, compared to mice without MAIT cell transfer (**Fig. 6, A-C**), suggesting that MAIT-1 cells can indeed provide protection in their

own right, in the absence of several other immune elements. To further explore the role of individual cytokines produced by MAIT cells in protecting against systemic *F. tularensis* LVS infection, adoptive transfer of WT *vs* cytokine-deficient MAIT cells to *Rag2*$^{-/-}\gamma C^{-/-}$ mice was performed. WT or IL-17-deficient MAIT cells were able to significantly prolong survival of mice following infection, with some mice surviving up to 58 dpi (**Fig. 6, C**). In contrast, MAIT cells deficient in production of TNF, INFγ or GM-CSF were unable to provide protection, with mice succumbing to infection similarly to the untreated *Rag2*$^{-/-}\gamma C^{-/-}$ mice. This was consistent with the susceptibility of mice genetically deficient in individual cytokines (**Supplementary Table 1**). Together, these data show that MAIT-1 cells have the capacity to contribute to systemic protection against bacterial infection and this can be the difference between life and death in the absence of other arms of the immune system.

Systemically boosted MAIT-1 cells manifest vaccination potential against local and systemic pathogens.

We previously showed that MAIT cells can be primed, providing more rapid control of *Legionella longbeachae* infection in the lungs[12, 39]. In the *Legionella* infection model the majority of MAIT cells were MAIT-17[39]. To explore the potential of systemically boosting MAIT-1 cells as a component of vaccination, here an immunization scheme was developed to boost MAIT cells systemically prior to bacterial challenge. Modifying our previously reported methods [12, 38, 39], we used synthetic MAIT antigen 5-OP-RU administered intravenously together with CpG adjuvant (**Fig. 7, A**). This resulted in a significantly expanded MAIT-1 cell pool systemically (in liver, lungs and spleen) without significantly changing the total numbers of non-MAIT αβ T cells (**Fig. 7, A, and Supplementary Fig. 6**). Furthermore, the majority of MAIT cells boosted with this vaccination scheme had a MAIT-1 phenotype (**Fig. 7, B**), similar to the MAIT cell phenotype driven by systemic *F. tularensis* LVS infection (**Fig. 3 and 4**).

To test the protective capacity afforded by MAIT-1 cell vaccination, mice were then challenged with *F. tularensis* LVS i.v. as depicted in **Fig. 7, C**. Vaccinated mice were rested for a month to foster MAIT memory formation and to allow the immune system to return to homeostasis. Both the bacterial load and mouse survival were assessed independently. Vaccinated WT C57BL/6 mice showed a significant reduction in the bacterial load in the liver and lungs at 3 and 5 dpi compared to unvaccinated mice, CpG only treated mice or vaccinated *Mr1*$^{-/-}$ mice (**Fig. 7, D, E**). Thus, our data show that a systemic vaccination scheme that targets MAIT cells can result in earlier clearance of bacteria. Consistent with the stronger MAIT cell response, vaccinated mice also showed enhanced survival of otherwise lethal *F. tularensis* infection (**Fig. 7, F**). We next assessed whether systemic

MAIT cells boosting could provide enhanced protection when challenged with a different bacterial pathogen. For this we used intranasal infection with *L. longbeachae.* The bacterial load in the lungs of mice at 5 and 7 post-challenge (intranasally), were significantly lower in vaccinated C57BL/6 mice than in the three control groups (**Fig. 7, G**) indicating that vaccination to boost MAIT cells can provide a level of protection against unrelated bacterial pathogens.

DISCUSSION

Our data show that MAIT cells respond in several organs and in the blood during systemic infection of mice with *F. tularensis* LVS. Regardless of delivery route, the infection resulted in bacterial replication in several organs and significant accumulation of MAIT-1 cells was observed in the liver, lungs, kidney, spleen and blood. As seen previously in lung infections we showed here that MAIT-1 cells are capable of protecting in multiple organs. Systemic priming of MAIT (programed to MAIT-1) cells could protect against two different bacteria at different sites.

An earlier study using intranasal delivery of *F. tularensis* LVS, showed significant MAIT cell expansion in the lungs at day 8 post infection[13]. Whilst that study defined MAIT cells as $CD4^{-}CD8^{-}$ T cells, here we have precisely identified MAIT cells using MR1:5-OP-RU tetramers, allowing us to detect MAIT cell accumulation as early as 4 dpi, with the peak of MAIT cell numbers observed at day 6 post-infection in most organs. MAIT cells are considered to bridge innate and adaptive immunity[42] consistent with our finding that compared with WT mice, an increased bacterial burden occurred earlier in *Mr1*$^{-/-}$ mice lacking MAIT cells. However, in both WT and *Mr1*$^{-/-}$ mice, bacteria were cleared to undetectable levels by 12 days post-infection, suggesting that other immune players, such as conventional T cells, also play an important role. Importantly, in the case of severe systemic infection (i.e. with a higher inoculum dose), or in the absence of other immunity (i.e. in *Rag2*$^{-/-}\gamma C^{-/-}$ mice) MAIT cell-mediated protection became of life or death importance.

Mouse MAIT cells were previously reported to egress the thymus with mutually-exclusive MAIT-1 or MAIT-17 effector phenotypes[43, 44], which correlate with T-bet and RORγt expression, respectively. In naïve mice, we observed a skewed composition of transcriptional expression according to tissue sites; with greater proportions of MAIT-1 cells in the liver, MAIT-17 cells in the lungs and similar proportions of MAIT-1 and MAIT-17 cells in the kidney, spleen and blood. Consistent with previous reports[43, 44, 45], this observation strongly suggests tissue specific imprints can favour one phenotype of MAIT cells. Surprisingly, infection with *F. tularensis* LVS resulted in a marked polarization to a MAIT-1 response, regardless of the tissue location. For example, naïve lung MAIT cells display a predominant MAIT-17 phenotype and express high levels of IL-17[12, 37]. However, upon *F. tularensis*

LVS infection, almost all MAIT cells in the lungs were T-bet^{+}, as distinct from the response to *Legionella* infection seen previously where MAIT cells from infected lungs were mostly MAIT-1/17 (T-bet^{+}/RORγt^{+} double positive)[12, 37]. The moderate skewing of liver MAIT cell population to MAIT-1 in naïve mice was further consolidated to >95% T-bet^{+} after *F. tularensis* infection. In a previous study, elevated IL-17A gene transcription was detected in total lung tissue of WT compared to *Mr1*$^{-/-}$ mice following pulmonary *F. tularensis* LVS infection[13]. However, here, using intracellular cytokine staining, we did not observe an increase in IL-17 production in the lungs by MAIT cells. Thus, in addition to tissue-specific cues, polarization signals from pathogens drive different MAIT cell responses, particularly during acute infection. It is unclear from the current study, whether polarised MAIT cell populations resulted from a preferential expansion, recruitment, or MAIT cell plasticity.

We previously showed that IFN-γ production from MAIT cells was necessary for their protective capacity in the absence of other T cells, B cells or NK cells[12]. However, in immune-sufficient mice, the contribution of MAIT cells is not clear. Previous studies suggested an indirect protection role of MAIT cell in pulmonary *F. tularensis* LVS infection, whereby MAIT cell-derived GM-CSF attracted monocyte maturation and subsequent conventional CD4^{+} T cell recruitment[13, 36]. Here, we observed GM-CSF production by MAIT cells in lungs, spleen and kidneys was detectable from day 6 and enhanced at day 14 post infection. However, significant proportions of MAIT cells also produced IFNγ and TNF, and adoptive transfer experiments showed that all three cytokines were indispensably important for the ability of MAIT cells to provide protection in an immunocompromised setting. Moreover, we found that mice lacking IFNγ or TNF were more susceptible than GM-CSF-deficient mice. Our data support a direct protection role for MAIT cells in this model where no other T cells are present.

MAIT cells have been termed “effector-memory” cells due to their expression, upon thymic egress, of a “memory-like” phenotype (CD62L^{low}, CD44^{high})[43]. We show here, that upon infection their initial response (accumulation and cytokine secretion) elicited a critical bridging protection role between innate and adaptive immunity. After the resolution of infection, a memory-like MAIT cell pool was formed and maintained at significantly higher frequency and with an infection-imprinted functional phenotype (MAIT-1) even after 100 days. A single vaccination reconstituted a similar memory-like MAIT cell pool post an infection (i.e. boosted number of MAIT-1 cells). The vaccinated mice controlled bacterial burdens faster and more efficiently than naïve, non-boosted mice. Thus, MAIT-1 cells show both an “innate-like” rapid response and adaptive memory-like features, consistent with our previous observations on MAIT-17/1 cells from respiratory infection models with *S.*

Typhimurium and *L. longbeachae*[12, 37] and hence this study amplifies our knowledge of both phenotypes of MAIT cells. Our data support the notion that both pathogen and host tissue signals appear to drive the polarisation of MAIT cells and contribute to the formation of the memory MAIT pool.

The augmented number and longevity of the expanded MAIT cell population and altered functional phenotype (MAIT-1) post infection support the concept of MAIT cell memory induction, and hence their potential as a vaccine target. Our vaccination and challenge data indeed provide proof-of-concept evidence that MAIT-1 cells that are systemically boosted in number and polarised in function can confer better protection against different pathogens at different sites; *F. tularensis* LVS systemic infection and *L. longbeachae* pulmonary infection. Our finding potentiates MAIT cells as a target to develop universal MAIT cell based immune interventions, including against antibiotic resistant pathogens.

METHODS

Mice. All mice were bred and housed in the Biological Research Facility of the Peter Doherty Institute for Infection and Immunity (Melbourne, Victoria, Australia). *Mr1*$^{-/-}$ mice were generated as previously described[46] by breeding *Vα19iCα*$^{-/-}$*Mr1*$^{-/-}$ mice[47] (from Susan Gilfillan, Washington University, St Louis School of Medicine, St Louis, MO) with C57BL/6 mice and inter-crossing of F1 mice. The genotype was determined by tail DNA PCR at the MR1 locus as previously described[46]. Mice aged 6–12 weeks were used in experiments, after approval by the University of Melbourne Animal Ethics Committee.

Compounds, immunogens and tetramers. 5-OP-RU was prepared as described previously[48]. Ac-6-FP was purchased from Shircks laboratories. CpG combo (CpG B and CpG P together), sequence: T*C*G*T*C*G*T*T*T*T*G*T*C*G*T*T*T*T*T*G*T*C*G*T*TT*CG*T* CG*A*CG*A*T*CG*G*C*G*CG*C*G*C*C*G (*phosphorothioate linkage) non-methylated cytosine-guanosine oligonucleotides was purchased from Integrated DNA Technologies, Singapore). Murine MR1 and β2-microglobulin genes were expressed in *Escherichia coli* purified from inclusion bodies, and refolded and purified as described previously[14, 49]. MR1:5-OP-RU and MR1:6-FP tetramers were generated as described previously[50].

Bacterial strains. Cultures of *F. tularensis* LVS were grown in 10 ml of brain heart infusion (BHI) broth for 16-18 h at 37 °C with shaking at 180 rpm, or on Cysteine Heart Agar (CYHA) plates containing 10 μg/ml ampicillin, 7.5 μg/ml colistin and 4 μg/ml trimethoprim for 4 days. For the

infecting inoculum, with the estimation that 1 OD_{600}=2.4x10^9/ml, bacteria from overnight culture were washed and diluted in phosphate buffered saline (PBS) for instillation to mice. A sample of inoculum was plated onto cysteine heart agar plates with appropriate antibiotics (as above mentioned) for verification of bacterial concentration by counting colony-forming units (CFU). *Legionella longbeachae* NSW150 was grown in buffered yeast extract (BYE) broth or agar plates supplemented with streptomycin (50 μg/ml).

Inoculation of and assessment of infected mice. *F. tularensis* LVS was delivered by intravenous (i.v.) injection via the tail vein (10 - 3x10^4 CFU in 200 μl PBS), intranasally (i.n. 50-200 CFU in 50 μl PBS), intratracheally (i.t. 10-50 CFU in 50 μl PBS), intraperitoneally (i.p. 20-60 CFU in 100 μl PBS) or subcutaneously (s.c. 5x10^2 - 5x10^5 CFU in 50 μl PBS). *L. longbeachae* NSW150 was delivered by intranasal instillation (i.n. 10^4 CFU in 50 μl PBS). Detailed protocols for inoculum preparation and i.n. instillation were described elsewhere[51]. Mice were weighed daily and assessed for visual signs of clinical disease, including inactivity, ruffled fur, labored breathing, and huddling behavior. Animals that had lost ≥20% of their original body weight and/or displayed evidence of pneumonia were euthanized.

Determination of bacterial counts in infected organs. Bacterial colonization was determined by counting CFU obtained from plating homogenized organs in duplicate, or 100 μl whole blood, from infected mice (5 per group) on buffered charcoal yeast extract agar containing 30 μg/ml streptomycin and colonies counted after 4 days at 37°C under aerobic conditions.

Vaccination: Age and gender matched C57BL/6 and *Mr1*$^{-/-}$ mice were inoculated (i.v.) with 10 nmol CpG together with 5-OP-RU (200 μl 1 nM) on day 0, followed by three additional 5-OP-RU injections at day 1, 3 and 5. Control mouse groups included untreated C57BL/6 and CpG alone vaccinated. Immunised mice were left for 4 weeks prior to challenge with either *F. tularensis* LVS or *L. longbeachae*.

Preparation of cells for flow cytometry. Detailed protocols for preparation of samples for flow cytometry from various organs and blood, were described elsewhere[51]. Briefly, for lungs perfusion through the heart was performed with 10 ml cold PBS, and lung single cell suspensions were prepared by finely chopping the lungs, followed by collagenase (type IV) digestion and red blood cell (RBC) lysis. Liver MAIT cells were prepared after by portal vein perfusion with 10 ml cold PBS, and pushing the liver tissue through 70 μm cell strainers, followed by gradient (33.75%:70% Percoll)

centrifugation to enrich lymphocytes, and RBC lysis. For blood, MAIT cells were analysed from 200 µl whole blood after RBC lysis. The absolute numbers of MAIT and non-MAIT T cells were calculated with reference to the number of counting beads (Sphero Rainbow Calibration Particles, BD Biosciences) added to each sample prior flow cytometry.

MAIT cell preparation for cell sorting and adoptive transfer. As MAIT cell frequencies are low in naïve mice, prior to adoptive transfer experiments MAIT cell populations were expanded in WT (C57BL/6) or cytokine KO mice by vaccination (as above) to increase MAIT cell numbers. After 7 days, single cells were prepared from the liver live $CD3^+CD45^+$MR1-5-OP-RU tetramer$^+$ cells sorted using a BD FACS Aria III. Detailed protocols for preparation of samples for FACS sorting are described elsewhere[51]. 10^5 MAIT cells were injected into the tail veins of recipient mice which then received 0.1 mg each of anti-CD4 (GK1.5) and anti-CD8 (53.762) mAb i.p on days 2 and either 5 or 6 to control residual conventional T cells. Mice were rested for 2 weeks post transfer to allow full expansion of the MAIT cell population prior to subsequent infectious challenge.

Antibodies and flow cytometry. Antibodies against murine CD4 (GK1.5, APC-Cy7), CD19 (1D3, PerCP-Cy 5.5), CD45.2 (104, FITC), IFNγ (XMG1.2, PE-Cy7), Ly6G (IA8, PECy7), TCRβ (H57-597, APC or PE), TNF (MP6-XT22, PE), GM-CSF (MP1-22E9, PE) and IL-17A (TC11-18H10, PE) were purchased from BD (Franklin Lakes, NJ). Antibodies against CD8a (53-6.7, PE), PLZF (Mags.21F7, PE), RORγt (B2D, APC), T-bet (4B10, PE-Cy7) and MHCII (M5/114.15.2, AF700) were purchased from eBioscience (San Diego, CA). Abs against CD19 (6D5, BV510), F4/80 (BM8, APC), CD11b (M1/70, FITC), CD11c (N418, BV786), CD31 (PCAM, MEC13.3, PerCPCy5.5), CD62L (Mel-14, FITC), CD64 (X54-5/71, BV711), CD146 (ME-9F1, PerCPCy5.5), CD326 (G8.8, EpCAM, APC-Cy7) were purchased from Biolegend (San Diego, CA). Blocking Ab (26.5: anti human MR1 MoAb or 8F2.F9: anti-mouse MR1 MoAb) and isotype controls (3E12, 8A5) were prepared in house. To block non-specific staining, cells were incubated with MR1-6FP tetramer and anti-Fc receptor (2.4G2) for 15 min at room temperature and then incubated at room temperature with Ab/tetramer cocktails in PBS/2% fetal calf serum. 7-aminoactinomycin D (5 µl per sample) was added for the last 10 min.

Cells were fixed with 1% paraformaldehyde prior to analysis on LSRII or LSR Fortessa or Canto II (BD Biosciences) flow cytometers. For intracellular cytokine staining Golgi plug (BD Biosciences) was used during all processing steps. Cells stimulated with PMA (phorbol 12-myristate 13-acetate;)/ionomycin (20 ng/ml, 1 µg/ml, respectively) for 3 h at 37 °C were included as positive controls. Surface staining was performed at 37 °C, and cells were stained for intracellular cytokines

using the BD Fixation/Permeabilization Kit (BD, Franklin Lakes, NJ) or transcription factors using the transcription buffer staining set (eBioscience) according to the manufacturers' instructions.

Statistical analysis. Statistical tests were performed using the Prism GraphPad software (version 7.0 La Jolla, CA). Comparisons between groups were performed using Student's t-tests or ANOVA tests as appropriate unless otherwise stated. Survival curves were compared using the Log-rank (Mantel-Cox) test for multiple groups. Flow cytometric data analysis was performed with FlowJo10 software (Ashland, OR).

AUTHOR CONTRIBUTIONS

ZZ and MS are joint first authors and designed, performed and analyzed data from the experiments; TZ, HW, TP, XL, BM, AN, DF, SE, JR, JMc, AJ and ZC performed experiments, provided key reagents, analyzed data and/or provided intellectual input; AC and ZC are joint senior and corresponding authors.

ACKNOWLEDGEMENTS

This research was supported by a Program Grant (1113293) and Project Grant (1120467) from the National Health and Medical Research Council of Australia (NHMRC). AJC is supported by a Future Fellowship (FT160100083) from the Australian Research Council (ARC). SBGE is supported by a DECRA Fellowship (DE170100407, ARC). DPF was supported by an NHMRC Senior Principal Research Fellowship (1117017). We thank Dr Wei-Jen Chua and Prof Ted Hansen for their kind provision of the 26.5 mAb and Prof. Dale Godfrey for critical discussion on this manuscript. *F. tularensis* LVS and *L. longbeachae* were kindly provided by Dr. Thomas J Inzana (Virginia Tech, USA) and Dr. Hayley Newton (University of Melbourne, Doherty Institute, Australia), respectively.

COMPETING INTERESTS

AC, ZC, SE, DF and JM. are inventors on patents describing MR1 tetramers and MAIT cell antigens. The other authors declared no conflict of interest.

DATA AVAILABILITY

REFERENCES

Uncategorized References

1. Ventola CL. The antibiotic resistance crisis: part 1: causes and threats. *P T* **40**, 277-283 (2015).

2. Hall MJ, Williams SN, DeFrances CJ, Golosinskiy A. Inpatient care for septicemia or sepsis: a challenge for patients and hospitals. *NCHS Data Brief*, 1-8 (2011).

3. Heyland DK, Hopman W, Coo H, Tranmer J, McColl MA. Long-term health-related quality of life in survivors of sepsis. Short Form 36: a valid and reliable measure of health-related quality of life. *Crit Care Med* **28**, 3599-3605 (2000).

4. Iwashyna TJ, Netzer G, Langa KM, Cigolle C. Spurious inferences about long-term outcomes: the case of severe sepsis and geriatric conditions. *Am J Respir Crit Care Med* **185**, 835-841 (2012).

5. Turnbull IR*, et al.* Effects of aging on the immunopathologic response to sepsis. *Crit Care Med* **37**, 1018-1023 (2009).

6. Fleischmann C*, et al.* Assessment of Global Incidence and Mortality of Hospital-treated Sepsis. Current Estimates and Limitations. *Am J Respir Crit Care Med* **193**, 259-272 (2016).

7. Thampy LK*, et al.* Restoration of T Cell function in multi-drug resistant bacterial sepsis after interleukin-7, anti-PD-L1, and OX-40 administration. *PLoS One* **13**, e0199497 (2018).

8. Gherardin NA*, et al.* Human blood MAIT cell subsets defined using MR1 tetramers. *Immunol Cell Biol*, (2018).

9. Gold MC, Lewinsohn DM. Co-dependents: MR1-restricted MAIT cells and their antimicrobial function. *Nat Rev Microbiol* **11**, 14-19 (2013).

10. Lepore M*, et al.* Parallel T-cell cloning and deep sequencing of human MAIT cells reveal stable oligoclonal TCRbeta repertoire. *Nat Commun* **5**, 3866 (2014).

11. Reantragoon R*, et al.* Antigen-loaded MR1 tetramers define T cell receptor heterogeneity in mucosal-associated invariant T cells. *J Exp Med* **210**, 2305-2320 (2013).

12. Wang H*, et al.* MAIT cells protect against pulmonary Legionella longbeachae infection. *Nat Commun* **9**, 3350 (2018).

13. Meierovics A, Yankelevich WJ, Cowley SC. MAIT cells are critical for optimal mucosal immune responses during in vivo pulmonary bacterial infection. *Proc Natl Acad Sci U S A* **110**, E3119-3128 (2013).

14. Kjer-Nielsen L*, et al.* An overview on the identification of MAIT cell antigens. *Immunol Cell Biol* **96**, 573-587 (2018).

15. Hartmann N*, et al.* Riboflavin Metabolism Variation among Clinical Isolates of Streptococcus pneumoniae Results in Differential Activation of Mucosal-associated Invariant T Cells. *Am J Respir Cell Mol Biol* **58**, 767-776 (2018).

16. Kurioka A*, et al.* Diverse Streptococcus pneumoniae Strains Drive a Mucosal-Associated Invariant T-Cell Response Through Major Histocompatibility Complex class I-Related Molecule-Dependent and Cytokine-Driven Pathways. *J Infect Dis* **217**, 988-999 (2018).

17. Le Bourhis L*, et al.* MAIT cells detect and efficiently lyse bacterially-infected epithelial cells. *PLoS Pathog* **9**, e1003681 (2013).

18. Jahreis S*, et al.* Human MAIT cells are rapidly activated by Aspergillus spp. in an APC-dependent manner. *Eur J Immunol* **48**, 1698-1706 (2018).

19. Dias J, Leeansyah E, Sandberg JK. Multiple layers of heterogeneity and subset diversity in human MAIT cell responses to distinct microorganisms and to innate cytokines. *Proc Natl Acad Sci U S A* **114**, E5434-E5443 (2017).

20. Coulter F*, et al.* IL-17 Production from T Helper 17, Mucosal-Associated Invariant T, and gammadelta Cells in Tuberculosis Infection and Disease. *Front Immunol* **8**, 1252 (2017).

21. Gold MC*, et al.* Human mucosal associated invariant T cells detect bacterially infected cells. *PLoS Biol* **8**, e1000407 (2010).

22. Le Bourhis L*, et al.* Antimicrobial activity of mucosal-associated invariant T cells. *Nat Immunol* **11**, 701-708 (2010).

23. Leung DT*, et al.* Circulating mucosal associated invariant T cells are activated in Vibrio cholerae O1 infection and associated with lipopolysaccharide antibody responses. *PLoS Negl Trop Dis* **8**, e3076 (2014).

24. Pincikova T, Paquin-Proulx D, Moll M, Flodstrom-Tullberg M, Hjelte L, Sandberg JK. Severely Impaired Control of Bacterial Infections in a Patient With Cystic Fibrosis Defective in Mucosal-Associated Invariant T Cells. *Chest* **153**, e93-e96 (2018).

25. Salerno-Goncalves R*, et al.* Challenge of Humans with Wild-type Salmonella enterica Serovar Typhi Elicits Changes in the Activation and Homing Characteristics of Mucosal-Associated Invariant T Cells. *Front Immunol* **8**, 398 (2017).

26. Smith DJ, Hill GR, Bell SC, Reid DW. Reduced mucosal associated invariant T-cells are associated with increased disease severity and Pseudomonas aeruginosa infection in cystic fibrosis. *PLoS One* **9**, e109891 (2014).

27. van Wilgenburg B*, et al.* MAIT cells are activated during human viral infections. *Nat Commun* **7**, 11653 (2016).

28. Godfrey DI, Koay HF, McCluskey J, Gherardin NA. The biology and functional importance of MAIT cells. *Nat Immunol* **20**, 1110-1128 (2019).

29. Rha MS*, et al.* Human liver CD8+ MAIT cells exert TCR/MR1-independent innate-like cytotoxicity in response to IL-15. *J Hepatol*, (2020).

30. Gibbs A*, et al.* MAIT cells reside in the female genital mucosa and are biased towards IL-17 and IL-22 production in response to bacterial stimulation. *Mucosal Immunol* **10**, 35-45 (2017).

31. Hama I*, et al.* Different distribution of mucosal-associated invariant T cells within the human cecum and colon. *Cent Eur J Immunol* **44**, 75-83 (2019).

32. Chua WJ, Truscott SM, Eickhoff CS, Blazevic A, Hoft DF, Hansen TH. Polyclonal mucosa-associated invariant T cells have unique innate functions in bacterial infection. *Infect Immun* **80**, 3256-3267 (2012).

33. Sjostedt A. Tularemia: history, epidemiology, pathogen physiology, and clinical manifestations. *Ann N Y Acad Sci* **1105**, 1-29 (2007).

34. Dennis DT*, et al.* Tularemia as a biological weapon: medical and public health management. *JAMA* **285**, 2763-2773 (2001).

35. J. Wayne Conlan WC, Catharine M. Bosio, Siobhán C. Cowley, and Karen, Elkins L. Infection of Mice with Francisella as an Immunological Model. *Curr Protoc Immunol* **CHAPTER: Unit–19.14**, (2011).

36. Meierovics AI, Cowley SC. MAIT cells promote inflammatory monocyte differentiation into dendritic cells during pulmonary intracellular infection. *J Exp Med* **213**, 2793-2809 (2016).

37. Chen Z*, et al.* Mucosal-associated invariant T-cell activation and accumulation after in vivo infection depends on microbial riboflavin synthesis and co-stimulatory signals. *Mucosal Immunol* **10**, 58-68 (2017).

38. D'Souza C*, et al.* Mucosal-Associated Invariant T Cells Augment Immunopathology and Gastritis in Chronic Helicobacter pylori Infection. *J Immunol* **200**, 1901-1916 (2018).

39. Wang H*, et al.* IL-23 costimulates antigen-specific MAIT cell activation and enables vaccination against bacterial infection. *Sci Immunol* **4**, (2019).

40. Ibidapo-Obe O*, et al.* Mucosal-Associated Invariant T Cells Redistribute to the Peritoneal Cavity During Spontaneous Bacterial Peritonitis and Contribute to Peritoneal Inflammation. *Cell Mol Gastroenterol Hepatol* **9**, 661-677 (2020).

41. Mazurier F*, et al.* A novel immunodeficient mouse model--RAG2 x common cytokine receptor gamma chain double mutants--requiring exogenous cytokine administration for human hematopoietic stem cell engraftment. *J Interferon Cytokine Res* **19**, 533-541 (1999).

42. Toubal A, Nel I, Lotersztajn S, Lehuen A. Mucosal-associated invariant T cells and disease. *Nat Rev Immunol* **19**, 643-657 (2019).

43. Koay HF*, et al.* A three-stage intrathymic development pathway for the mucosal-associated invariant T cell lineage. *Nat Immunol* **17**, 1300-1311 (2016).

44. Legoux F, Gilet J, Procopio E, Echasserieau K, Bernardeau K, Lantz O. Molecular mechanisms of lineage decisions in metabolite-specific T cells. *Nat Immunol* **20**, 1244-1255 (2019).

45. Salou M*, et al.* A common transcriptomic program acquired in the thymus defines tissue residency of MAIT and NKT subsets. *J Exp Med*, (2018).

46. Chen X*, et al.* IL-17R-EGFR axis links wound healing to tumorigenesis in Lrig1(+) stem cells. *J Exp Med* **216**, 195-214 (2019).

47. Kawachi I, Maldonado J, Strader C, Gilfillan S. MR1-restricted V alpha 19i mucosal-associated invariant T cells are innate T cells in the gut lamina propria that provide a rapid and diverse cytokine response. *J Immunol* **176**, 1618-1627 (2006).

48. Mak JY*, et al.* Stabilizing short-lived Schiff base derivatives of 5-aminouracils that activate mucosal-associated invariant T cells. *Nat Commun* **8**, 14599 (2017).

49. Patel O*, et al.* Recognition of vitamin B metabolites by mucosal-associated invariant T cells. *Nat Commun* **4**, 2142 (2013).

50. Corbett AJ*, et al.* T-cell activation by transitory neo-antigens derived from distinct microbial pathways. *Nature* **509**, 361-365 (2014).

51. Chen Z, Wang, H., D'Souza, C., Koay, H.-F, Meehan, B., Zhao, Z., Pediongco, T., Shi, M., Zhu, T., Wang, B., Kjer-Nielsen, L., Eckle, S. B. G., Rossjohn, J., Fairlie, D. P., Godfrey, D. I., Strugnell, R. A., McCluskey, J., & Corbett, A. J. Characterization and purification of mouse mucosal-associated invariant T (MAIT) cells. *Current Protocols in Immunology* **127,**, (2019).

FIGURE LEGENDS

Figure 1. *Francisella tularensis* LVS activates MAIT reporter cells via MR1 *in vitro* and induces systematic MAIT cell expansion *in vivo*. (A) Jurkat.MAIT-AF7 and C1R.MR1 cells were co-incubated for 16 h with indicated amounts of *F. tularensis* lysate (in PBS), 5-OP-RU, acetyl-6-formylpterin (Ac-6-FP), or PBS. Activation was detected by staining with anti-CD69 antibody. Anti-MR1 antibody (26.5) or isotype control (W6/32) was added to C1R.MR1 cells 2 h prior to co-incubation. Experiments were performed in triplicate on 3 separate occasions with similar results. Data show mean fluorescence intensity (MFI) (mean ± SEM of 6 data points from 2 experiments). Statistical tests: One-way ANOVA comparing lysate groups with the PBS group and unpaired *t*-test comparing isotype control with Ab-blocked samples **P<0.01, ***P<0.001, ****P<0.0001. **(B)** Flow cytometry plots, and **(C)** MAIT cell percentage in αβ-T cells from liver, lung, spleen, kidney and blood (200 µl) of C57BL/6 mice either uninfected or intravenously infected with 10^4 CFU *F. tularensis* LVS for 14 days. **(D)** and **(E)** show absolute numbers of MAIT cells and non-MAIT αβ-T cells respectively, in liver, lung, spleen, kidney and blood (200 µl) of C57BL/6 mice either uninfected or intravenously infected, 14 days post infection. The experiment was performed twice with similar results. Data show mean ± SEM n=5 mice from one experiment. Statistical tests: Unpaired *t*-test comparing uninfected with infected mice. *P<0.05, **P<0.01, ***P<0.001, ****P<0.0001. The gating strategy for mouse MAIT cells is depicted in **Supplementary Fig. 1, A**.

Figure 2. Systemic and long-lasting expansion of MAIT cells in *F. tularensis* LVS infection. (A) Bacterial load (CFU/organ or CFU/100 µl blood) from C57BL/6 mice at indicated time points post infection i.v. with 2×10^4 CFU *F. tularensis* LVS. Pooled data are presented as mean ± SEM of n=6-20 mice per group. **(B-G)** Relative and absolute number of MAIT cells and non-MAIT αβ-T cells detected in various organs (as indicated) from naïve and infected mice at indicated time points post infection. Pooled data from 3 independent experiments (mean ± SEM, n= 7-17 mice per group). Statistical test: one-way ANOVA, *P<0.05, **P<0.01, ***P<0.001, ****P<0.0001. **(H)** Body weight was recorded daily and calculated in percentage relative to starting weight of the individual mouse. Data are presented as mean ± SEM (n=20 mice).

Figure 3. Cytokine profiling of MAIT cells upon *F. tularensis* LVS infection. (A) Representative flow cytometry plots showing intracellular cytokine staining for IFNγ of $TCR\beta^+$ lymphocytes from liver, lungs, spleen, and kidneys of uninfected and infected mice on 6, 14 and 100 dpi with 2×10^4 CFU *F. tularensis* LVS i.v, after 4 h of culture with brefeldin A and PMA/ionomycin stimulation. **(B-C)** Percentages of **(B)** IFNγ and (**C**) TNF, GM-CSF and IL-17-producing cells of gated MAIT

cells and non-MAIT αβ-T cells from liver, lungs, spleen, and kidneys from mice in (A). Pooled data 2 independent experiments with similar results (mean ± SEM, n=5-10 mice per group).

Figure 4. MAIT cells were polarised to functional MAIT-1 phenotype upon *F. tularensis* infection. A. Representative flow cytometry plots showing intranuclear staining for T-bet (representing Th1) and RORγt (Th17) in gated MAIT cells from the liver, lungs, spleen, kidneys and blood of naïve and infected mice on 6 and 100 dpi with 2×10^4 CFU *F. tularensis* LVS i.v. Number in quadrants represent cell percentage. **B.** Percentage of MAIT cells expressing combinations of T-bet and RORγt from the same mice in (A). Pooled data from 2 independent experiments (mean ± SEM, n= 5-10 mice per group).

Figure 5. MAIT cells optimized bacteria clearance systemically and afford greater survival after intravenous *F. tularensis* infection. (A-E) WT (C57BL/6) or *Mr1*$^{-/-}$ mice were infected i.v. with 2×10^4 CFU *F. tularensis* LVS. The bacterial burden (CFU) in the liver, lung, spleen, kidney and blood (100 μl) was assessed at the indicated dpi. 0 dpi was examined at 4 h after inoculation. Pooled data (mean ± SEM) from 2 independent experiments with similar results using 4-10 mice per group at each time point. Two-way ANOVA on log-transformed data. *P<0.05, **P<0.01, ***P<0.001, ****P<0.0001. **(F)** Survival of WT (C57BL/6) or *Mr1*$^{-/-}$ mice challenged with 2.5×10^4 CFU *F. tularensis* LVS. Log-rank test. **P<0.01.

Figure 6. MAIT cell-mediated protection requires IFN, TNF and GM-CSF. (A) MAIT cell percentage of αβ-T cells in the liver, and representative FACS plot showing intranuclear staining for T-bet and RORγt of MAIT cells from donor C57BL/6 mice vaccinated with CpG and 5-OP-RU i.v. for 7 days, prior cell sorting for adoptive cell transfer. Pooled data from 7 (nil) or 11 (vaccinated) mice from 3 independent experiments (mean ± SEM). Unpaired *t*-test. ****P<0.0001. **(B)** Schematic of protocol for MAIT cell adoptive transfer and *F. tularensis* LVS challenge: 10^5 liver MAIT cells from C57BL/6 (WT, shown in **A**), *Ifnγ*$^{-/-}$, *Tnf*$^{-/-}$, *Gm-csf*$^{-/-}$ or *Il-17*$^{-/-}$ mice vaccinated with CpG (10 nmol) and 5-OP-RU (10 μM) i.v. for 7 days were sorted by flow cytometry and transferred i.v. into *Rag2*$^{-/-}$*γC*$^{-/-}$ mice. The mice were treated with anti-CD4 and anti-CD8 mAb injection (i.p., 0.1 mg each) at days 1 and 3 post MAIT cell transfer to deplete contaminating conventional T cells. After two weeks, mice were infected with an otherwise lethal dose (20 CFU) of *F. tularensis* LVS i.v. **(C)** Survival of untreated *Rag2*$^{-/-}$*γC*$^{-/-}$ mice or *Rag2*$^{-/-}$*γC*$^{-/-}$ mice following transfer of MAIT cells from WT, *Ifnγ*$^{-/-}$, *Tnf*$^{-/-}$, *Gm-csf*$^{-/-}$ or *Il-17*$^{-/-}$ mice according to schematic shown in (B). Pooled data from 2 independent experiments with similar results (n=12-24 mice per group as indicated). Log-rank tests

(*Ifnγ*$^{-/-}$, *Tnf*$^{-/-}$, *Gm-csf*$^{-/-}$ and *Il-17*$^{-/-}$ groups were compared with WT group), ****P < 0.0001.

Figure 7. MAIT cell targeted vaccination delivers significant protection against both local and systemic bacterial pathogens. (A) MAIT cell number and **(B)** T-bet and RORγt phenotype of MAIT cells in liver and lungs of C57BL/6 mice 30 days after i.v. vaccination with 5-OP-RU and CpG (as depicted in C). Pooled data from 3 independent experiments with similar results (mean ± SEM. A: n=13-19 mice per group, B: n=9 mice per group). Unpaired *t*-test, ***P<0.001, ****P<0.0001. **(C)** Schematic flow chart for vaccination and challenge. Mice were administered with CpG (10 nmol) alone or CpG together with 2 nmol 5-OP-RU in 200 µl PBS at day 0) and 5-OP-RU (2 nmol in 200 µl PBS on day 1, 2 and 4). After 30 days mice were infected with 2.5×10^4 CFU of *F. tularensis* LVS i.v. or 10^4 CFU of *L. longbeachae* i.n. **(D-E)** Bacterial load in liver and lungs respectively, of unvaccinated WT (C57BL/6) mice (Nil, open diamond), mock vaccinated WT mice (CpG only, open circle), vaccinated *Mr1*$^{-/-}$ mice (CpG + 5-OP-RU, open square) and vaccinated WT mice (CpG + 5-OP-RU, filled circle) at indicated time points post *F. tularensis* challenge ($2.5x10^4$ CFU, i.v.). **(F)** Survival of mice vaccinated (as in **D, E** and **F**) after *F. tularensis* challenge ($3x10^4$ CFU, i.v.). **(G)** Bacterial load in lungs of mice vaccinated and challenged with *L. longbeachae* at indicated time points post *L. longbeachae* challenge. One-way ANOVA on log-transformed data (unvaccinated, CpG only and vaccinated *Mr1*$^{-/-}$ groups were compared with vaccinated WT group), *P<0.05, **P<0.01, ***P<0.001, ****P<0.0001. Pooled data from 3 independent experiments with similar results (mean ± SEM, n= 10 mice per group (D-E), 20 mice per group (F) or 12-18 mice per group (G)).

Figures

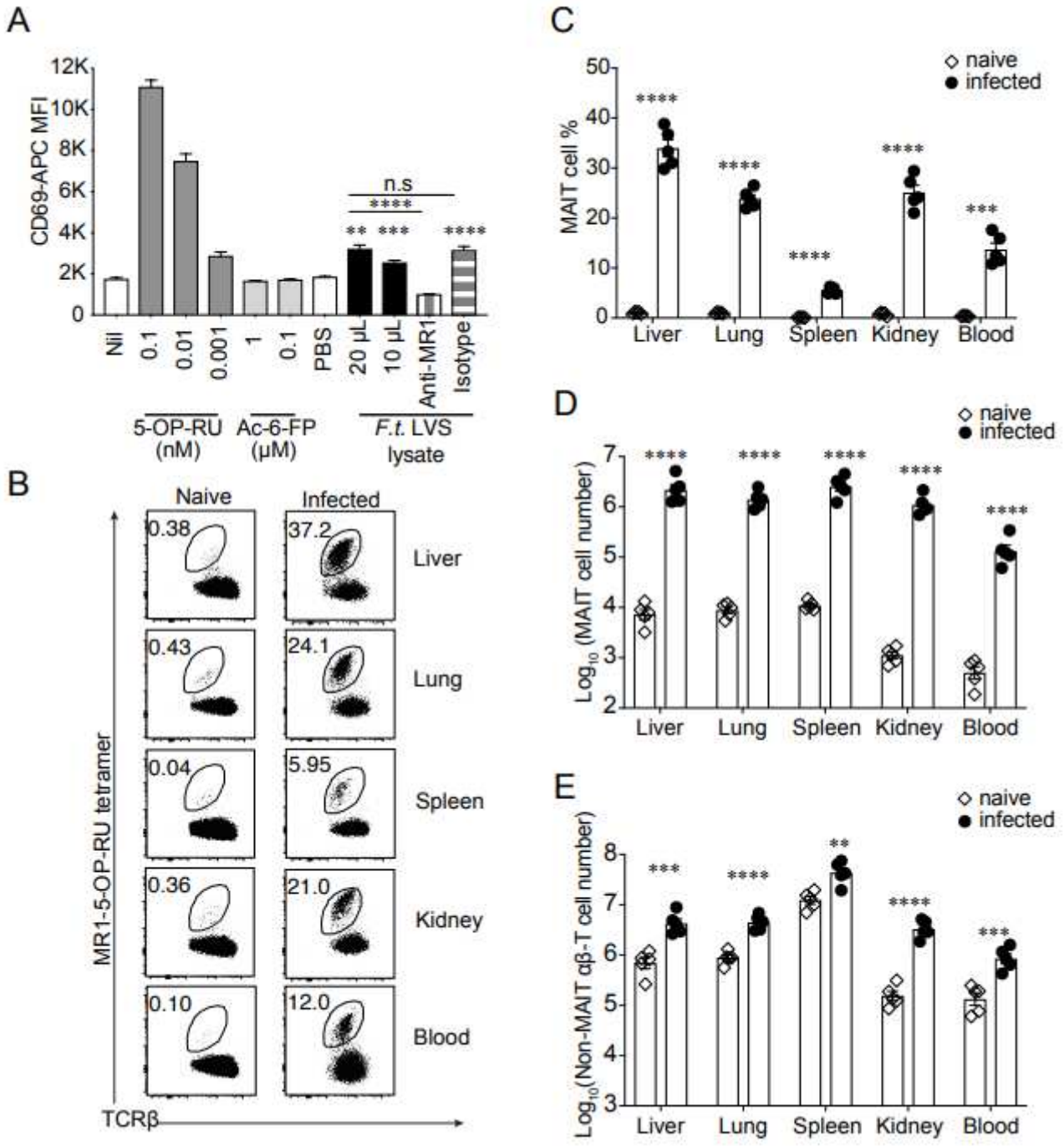

Figure 1

Francisella tularensis LVS activates MAIT reporter cells via MR1 in vitro and induces systematic MAIT cell expansion in vivo. (A) Jurkat.MAIT-AF7 and C1R.MR1 cells were coincubated for 16 h with indicated amounts of F. tularensis lysate (in PBS), 5-OP-RU, acetyl-6- formylpterin (Ac-6-FP), or PBS. Activation was detected by staining with anti-CD69 antibody. AntiMR1 antibody (26.5) or isotype control (W6/32) was

added to C1R.MR1 cells 2 h prior to coincubation. Experiments were performed in triplicate on 3 separate occasions with similar results. Data show mean fluorescence intensity (MFI) (mean ± SEM of 6 data points from 2 experiments). Statistical tests: One-way ANOVA comparing lysate groups with the PBS group and unpaired t-test comparing isotype control with Ab-blocked samples **P<0.01, ***P<0.001, ****P<0.0001. (B) Flow cytometry plots, and (C) MAIT cell percentage in ab-T cells from liver, lung, spleen, kidney and blood (200 µl) of C57BL/6 mice either uninfected or intravenously infected with 104 CFU F. tularensis LVS for 14 days. (D) and (E) show absolute numbers of MAIT cells and non-MAIT ab-T cells respectively, in liver, lung, spleen, kidney and blood (200 µl) of C57BL/6 mice either uninfected or intravenously infected, 14 days post infection. The experiment was performed twice with similar results. Data show mean ± SEM n=5 mice from one experiment. Statistical tests: Unpaired t-test comparing uninfected with infected mice. *P<0.05, **P<0.01, ***P<0.001, ****P<0.0001. The gating strategy for mouse MAIT cells is depicted in Supplementary Fig. 1, A.

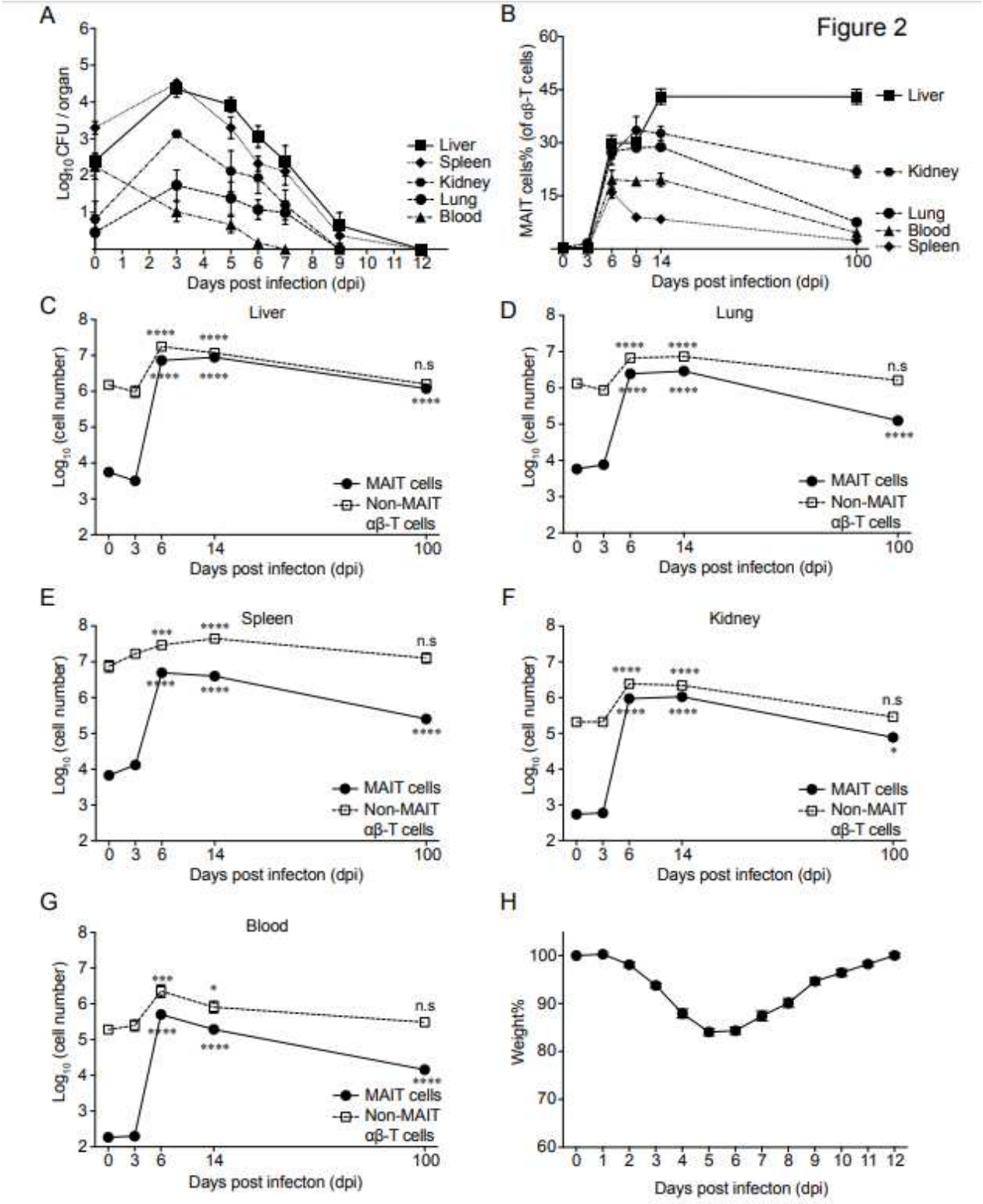

Figure 2

Systemic and long-lasting expansion of MAIT cells in F. tularensis LVS infection. (A) Bacterial load (CFU/organ or CFU/100 µl blood) from C57BL/6 mice at indicated time points post infection i.v. with 2×104 CFU F. tularensis LVS. Pooled data are presented as mean ± SEM of n=6- 20 mice per group. (B-G) Relative and absolute number of MAIT cells and non-MAIT ab-T cells detected in various organs (as indicated) from naïve and infected mice at indicated time points post infection. Pooled data from 3

independent experiments (mean ± SEM, n= 7-17 mice per group). Statistical test: one-way ANOVA, *P<0.05, **P<0.01, ***P<0.001, ****P<0.0001. (H) Body weight was recorded daily and calculated in percentage relative to starting weight of the individual mouse. Data are presented as mean ± SEM (n=20 mice).

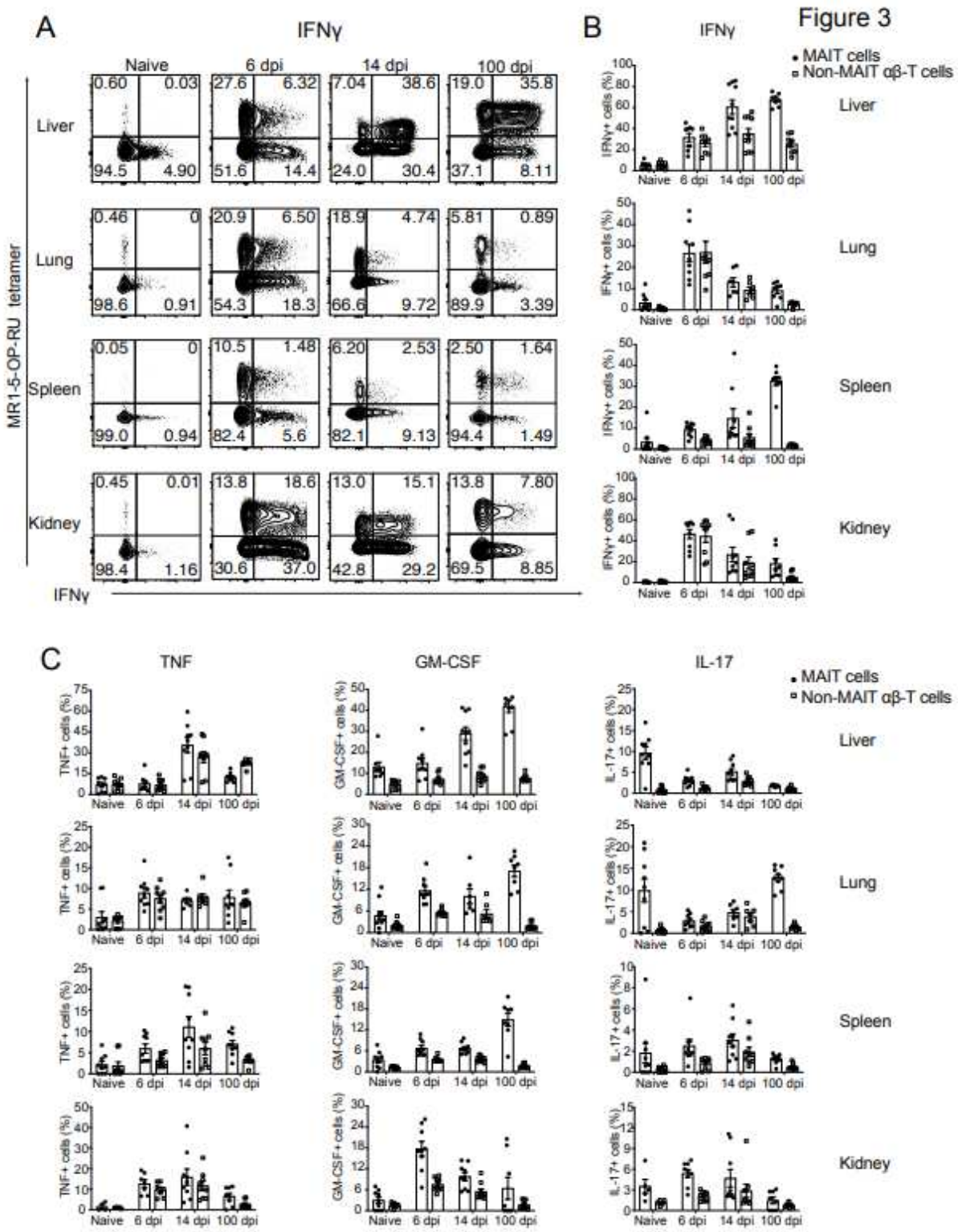

Figure 3

Cytokine profiling of MAIT cells upon F. tularensis LVS infection. (A) Representative flow cytometry plots showing intracellular cytokine staining for IFNg of TCRβ+ lymphocytes from liver, lungs, spleen, and kidneys of uninfected and infected mice on 6, 14 and 100 dpi with 2×104 CFU F. tularensis LVS i.v, after 4 h of culture with brefeldin A and PMA/ionomycin stimulation. (B-C) Percentages of (B) IFNg and (C) TNF, GM-CSF and IL-17-producing cells of gated MAIT cells and non-MAIT ab-T cells from liver, lungs, spleen, and kidneys from mice in (A). Pooled data 2 independent experiments with similar results (mean ± SEM, n=5-10 mice per group).

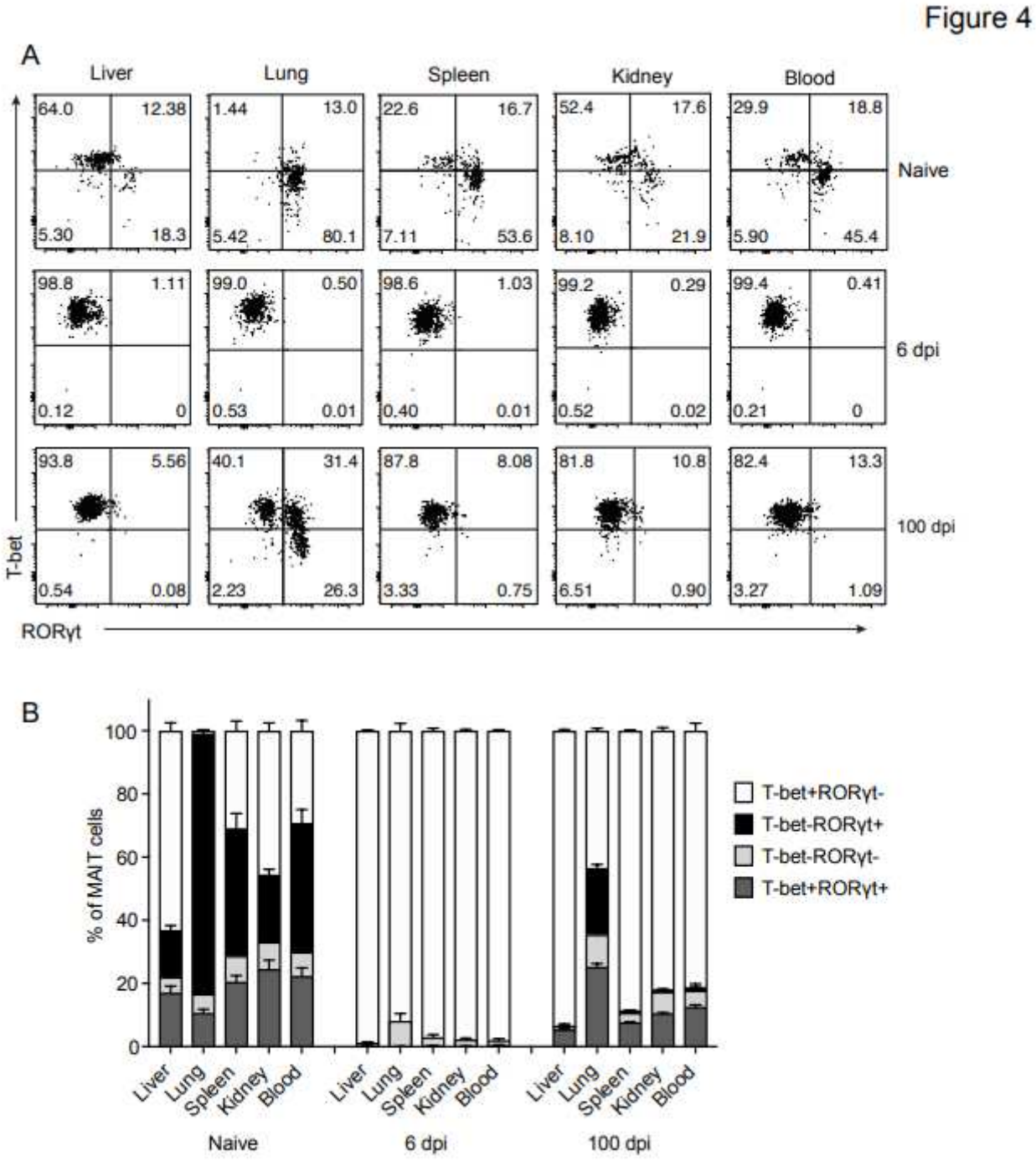

Figure 4

MAIT cells were polarised to functional MAIT-1 phenotype upon F. tularensis infection. A. Representative flow cytometry plots showing intranuclear staining for T-bet (representing Th1) and RORgt (Th17) in gated MAIT cells from the liver, lungs, spleen, kidneys and blood of naïve and infected mice on 6 and 100 dpi with 2×104 CFU F. tularensis LVS i.v. Number in quadrants represent cell percentage. B. Percentage of MAIT cells expressing combinations of Tbet and RORgt from the same mice in (A). Pooled data from 2 independent experiments (mean ± SEM, n= 5-10 mice per group).

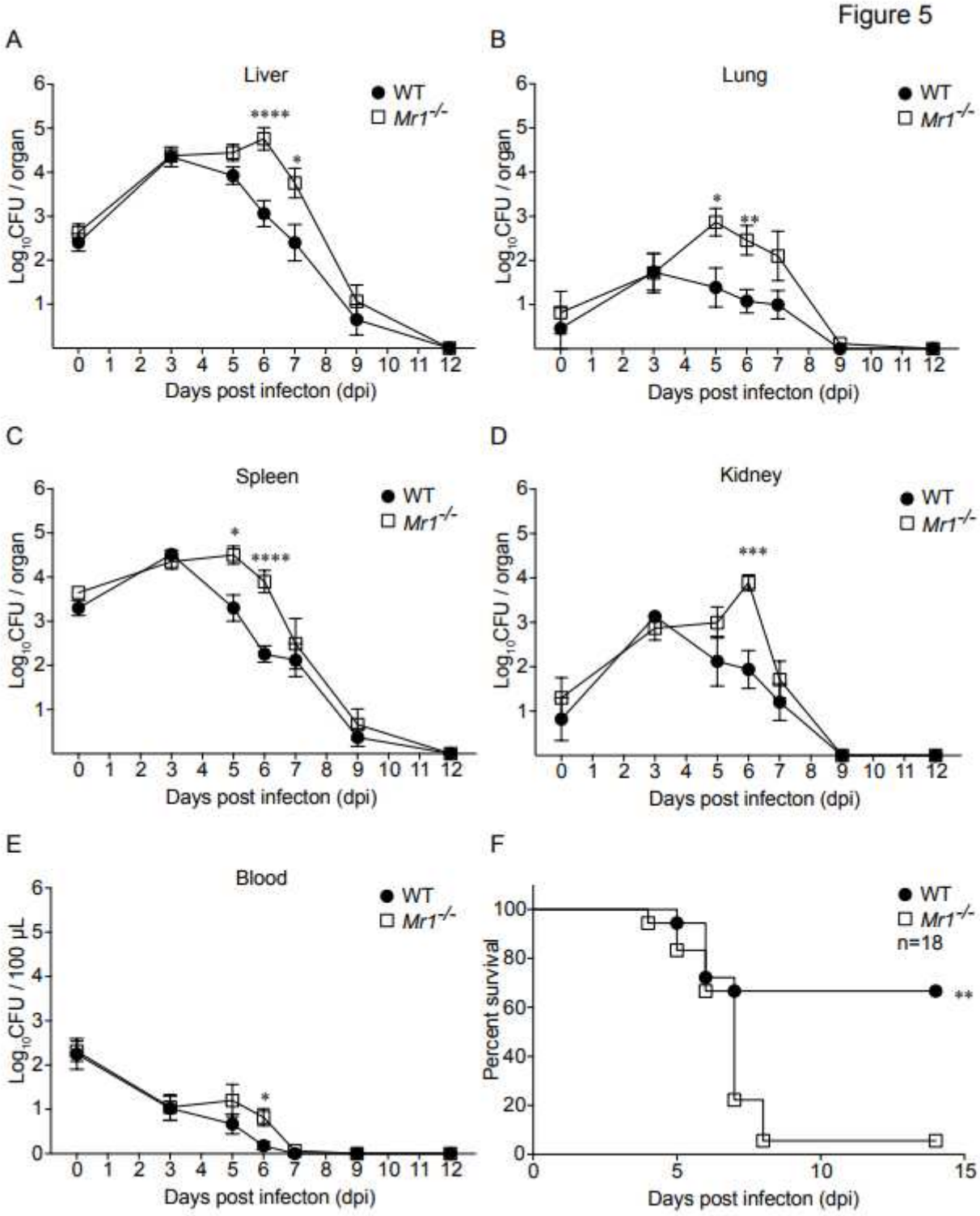

Figure 5

MAIT cells optimized bacteria clearance systemically and afford greater survival after intravenous F. tularensis infection. (A-E) WT (C57BL/6) or Mr1-/- mice were infected i.v. with 2×104 CFU F. tularensis LVS. The bacterial burden (CFU) in the liver, lung, spleen, kidney and blood (100 µl) was assessed at the indicated dpi. 0 dpi was examined at 4 h after inoculation. Pooled data (mean ± SEM) from 2 independent experiments with similar results using 4-10 mice per group at each time point. Two-way ANOVA on log-transformed data. *P<0.05, **P<0.01, ***P<0.001, ****P<0.0001. (F) Survival of WT (C57BL/6) or Mr1-/- mice challenged with 2.5×104 CFU F. tularensis LVS. Log-rank test. **P<0.01.

Figure 6

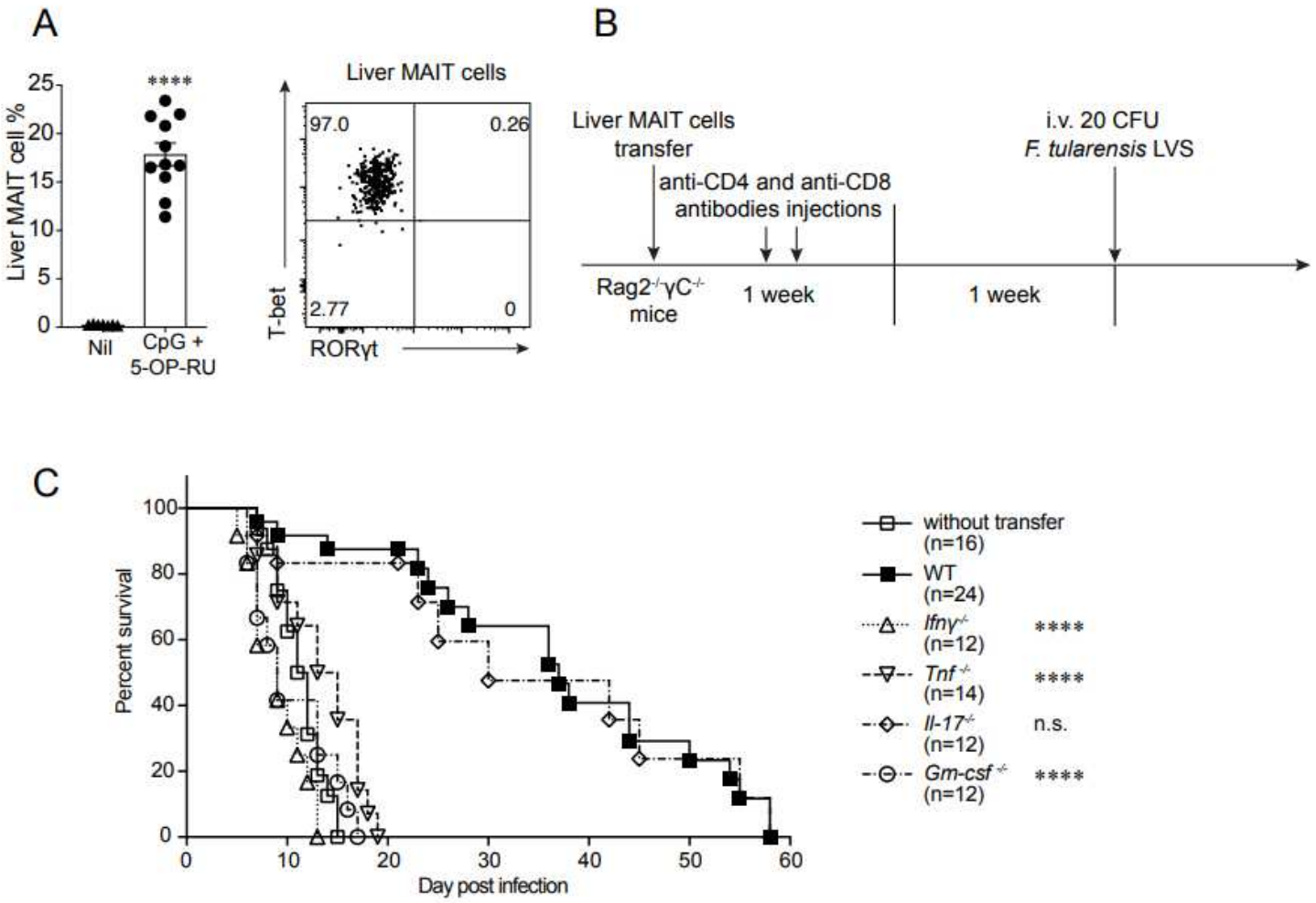

Figure 6

MAIT cell-mediated protection requires IFN, TNF and GM-CSF. (A) MAIT cell percentage of ab-T cells in the liver, and representative FACS plot showing intranuclear staining for T-bet and RORgt of MAIT cells from donor C57BL/6 mice vaccinated with CpG and 5-OP-RU i.v. for 7 days, prior cell sorting for adoptive cell transfer. Pooled data from 7 (nil) or 11 (vaccinated) mice from 3 independent experiments (mean ± SEM). Unpaired t-test. ****P<0.0001. (B) Schematic of protocol for MAIT cell adoptive transfer and F. tularensis LVS challenge: 105 liver MAIT cells from C57BL/6 (WT, shown in A), Ifng -/- , Tnf-/- , Gm-csf-/- or Il-17-/- mice vaccinated with CpG (10 nmol) and 5-OP-RU (10 µM) i.v. for 7 days were sorted by flow cytometry

and transferred i.v. into Rag2-/- gC-/- mice. The mice were treated with anti-CD4 and anti-CD8 mAb injection (i.p., 0.1 mg each) at days 1 and 3 post MAIT cell transfer to deplete contaminating conventional T cells. After two weeks, mice were infected with an otherwise lethal dose (20 CFU) of F. tularensis LVS i.v. (C) Survival of untreated Rag2-/- gC-/- mice or Rag2-/- gC-/- mice following transfer of MAIT cells from WT, Ifng -/- , Tnf-/- , Gm-csf-/- or Il-17-/- mice according to schematic shown in (B). Pooled data from 2 independent experiments with similar results (n=12-24 mice per group as indicated). Log-rank tests 20 (Ifng -/- , Tnf-/- , Gm-csf-/- and Il-17-/- groups were compared with WT group), ****P < 0.0001.

Figure 7

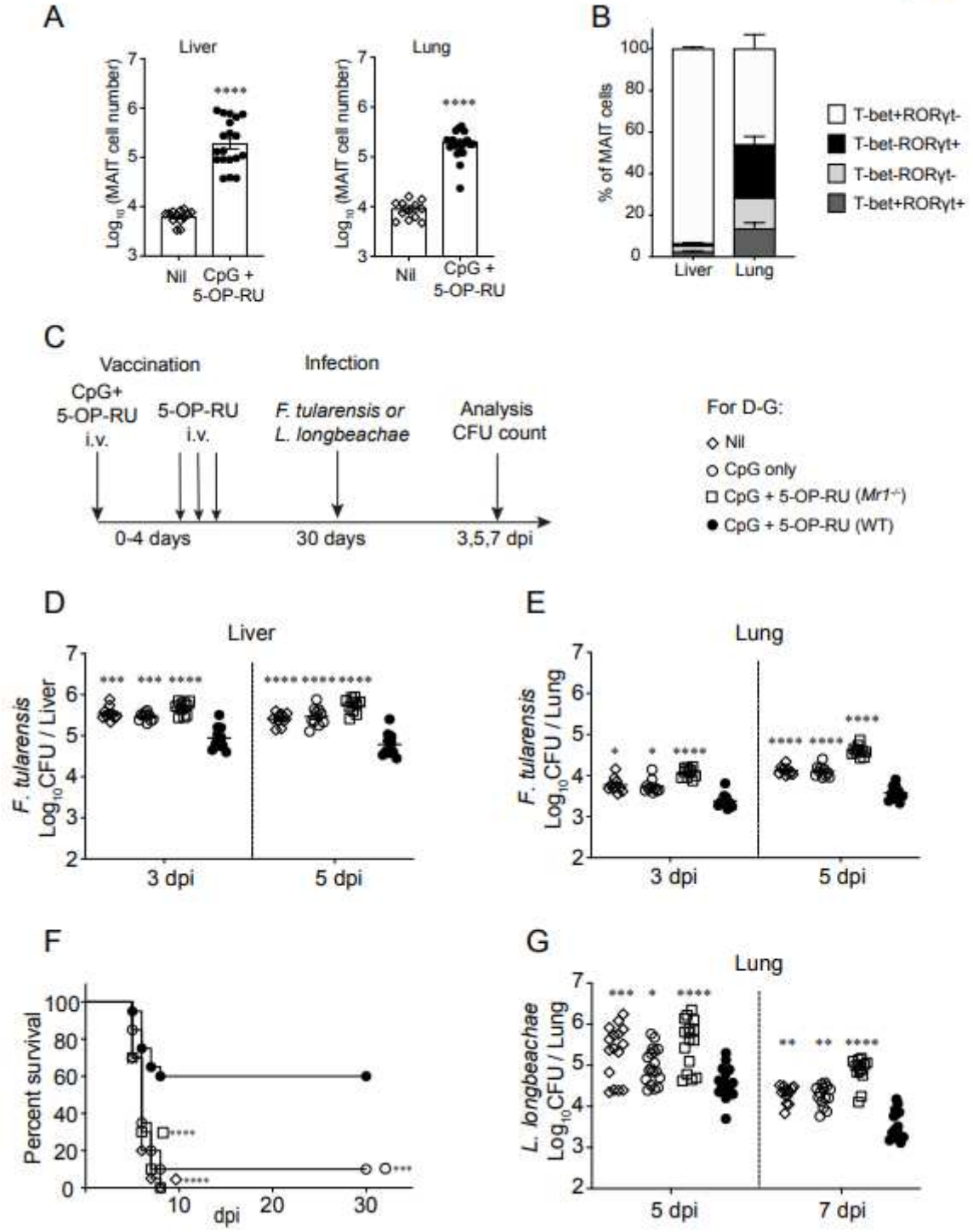

Figure 7

MAIT cell targeted vaccination delivers significant protection against both local and systemic bacterial pathogens. (A) MAIT cell number and (B) T-bet and RORgt phenotype of MAIT cells in liver and lungs of C57BL/6 mice 30 days after i.v. vaccination with 5-OP-RU and CpG (as depicted in C). Pooled data from 3 independent experiments with similar results (mean ± SEM. A: n=13-19 mice per group, B: n=9 mice per group). Unpaired t-test, ***P<0.001, ****P<0.0001. (C) Schematic flow chart for vaccination and challenge. Mice were administered with CpG (10 nmol) alone or CpG together with 2 nmol 5-OP-RU in 200 µl PBS at day 0) and 5-OP-RU (2 nmol in 200 µl PBS on day 1, 2 and 4). After 30 days mice were infected with 2.5×104 CFU of F. tularensis LVS i.v. or 104 CFU of L. longbeachae i.n. (D-E) Bacterial load in liver and lungs respectively, of unvaccinated WT (C57BL/6) mice (Nil, open diamond), mock vaccinated WT mice (CpG only, open circle), vaccinated Mr1-/- mice (CpG + 5-OP-RU, open square) and vaccinated WT mice (CpG + 5- OP-RU, filled circle) at indicated time points post F. tularensis challenge (2.5x104 CFU, i.v.). (F) Survival of mice vaccinated (as in D, E and F) after F. tularensis challenge (3x104 CFU, i.v.). (G) Bacterial load in lungs of mice vaccinated and challenged with L. longbeachae at indicated time points post L. longbeachae challenge. One-way ANOVA on log-transformed data (unvaccinated, CpG only and vaccinated Mr1-/- groups were compared with vaccinated WT group), *P<0.05, **P<0.01, ***P<0.001, ****P<0.0001. Pooled data from 3 independent experiments with similar results (mean ± SEM, n= 10 mice per group (D-E), 20 mice per group (F) or 12-18 mice per group (G)).

Supplementary Files

This is a list of supplementary files associated with this preprint. Click to download.

- ZhaoetalFiguresSuppNComms.pdf